JOURNAL OF GUIDANCE, CONTROL, AND DYNAMICS
Vol. 18, No. 4, July–August 1995

# Evaluation of Optimal-Guidance Algorithm for Aeroassisted Orbit Transfer

N. Melamed* and A. J. Calise†
*Georgia Institute of Technology, Atlanta, Georgia 30332*

**In this paper we perform an evaluation of a guidance algorithm for aeroassisted orbit transfer based on the method of matched asymptotic expansions (MAEs). It is shown that, by exploiting the structure of the matched asymptotic expansion solution procedure, the original problem, which requires the solution of a set of 20 implicit algebraic equations, can be reduced to a problem of 6 implicit equations in 6 unknowns. Guidance law implementation entails treating the current state as a new initial state and repetitively solving the MAE problem to obtain the feedback controls.**

## I. Introduction

AN objective in any guidance study related to aeroassisted orbit transfer vehicles is the development of solutions that are implementable in real time and on board the vehicle. Therefore, solutions that are both near optimal and that require a minimum of computation are of primary interest. In this paper we perform a detailed evaluation of a guidance algorithm for aeroassisted inclination change with minimum energy loss that was first developed in Ref. 1. The algorithm is based on the method of matched asymptotic expansions (MAEs). The interested reader is referred to Ref. 1 for the background on this problem and the references there that are directly related to this research.

The paper begins with a summary of the results in Ref. 1. This is followed by a description of the zero-order MAE solution procedure, which makes use of a unique approach for solving the algebraic equations in Ref. 1. The paper concludes by giving some representative results wherein the solution is examined both in an open-loop setting and in the setting of closed-loop guidance.

## II. Zero-Order MAE Solution

A complete set of integrals for the state and costate equations for the problem of inclination change with minimum energy loss were presented in Ref. 1. Enforcing the MAE matching conditions, boundary conditions, and optimality conditions results in a set of 20 nonlinear algebraic equations. The solution of these equations provides the information needed to form a guidance algorithm that is uniformly valid to $(\mathcal{O}\varepsilon)$, where $\varepsilon$ is a perturbation parameter defined below.

The reduced three-dimensional point-mass equations of motion for a lifting vehicle over a spherical nonrotating planet are given by

$$\frac{du}{dh} = -\frac{Bu(1+\lambda^2)e^{-h/\varepsilon}}{\varepsilon E^* \sin\gamma} - \frac{2}{(1+h)^2} \tag{1}$$

$$\frac{d\gamma}{dh} = B\lambda\frac{\cos\mu e^{-h/\varepsilon}}{\varepsilon\sin\gamma} + \left(\frac{1}{1+h} - \frac{1}{u(1+h)^2}\right)\cot\gamma \tag{2}$$

$$\frac{d\psi}{dh} = B\lambda\frac{\sin\mu e^{-h/\varepsilon}}{\varepsilon\sin\gamma\cos\gamma} \tag{3}$$

where the parameter $\varepsilon$ is the ratio of the atmospheric scale height $(1/\beta)$ to the minimum trajectory radius $r_s$. For Earth the value of $\varepsilon$ is approximately 1/900. The definitions for the remaining variables are given below. Using the definition of $u$ given in Eq. (12) below, the objective of minimizing energy loss can be equivalently expressed as

$$\max\{J\}, \qquad J = u_f \tag{4}$$

Assume that the initial conditions $u_i$, $\gamma_i$, and $\psi_i$ are given, along with the initial radius $r_i$. For the purpose of exposition, assume that $\gamma_f$, $\psi_f$, and the final radius $r_f$ are given. The corresponding transversality condition is $P_u^c(h_f) = 1$.

The controls are the normalized lift coefficient $\lambda$ and the bank angle $\mu$, which are assumed not to be beyond their limits. The optimal control is obtained as a function of the state and costate variables by solving the optimality conditions. The resulting expressions are

$$\begin{aligned} \tan\mu &= P_\psi/P_\gamma\cos\gamma, \\ \lambda &= E^*(P_\gamma\cos\mu + P_\psi\sin\mu/\cos\gamma)/2uP_u \end{aligned} \tag{5}$$

where $p_u$, $p_\gamma$, and $p_\psi$ are the associated costate variables. To determine uniquely the quantities $\sin\mu$ and $\cos\mu$ used in Eqs. (1–3), an appropriate statement was implemented in the computer code that takes into account the quadrant of the angle $\mu$.

The zero-order equations for the outer problem can be obtained by simply taking the limit as $\varepsilon$ approaches zero on the right-hand side of Eqs. (1–3). The general solution for the outer system to zero order in $\varepsilon$ is given by

$$u_0^o(h) = 2[c_1 + 1/(1+h)] \tag{6}$$

$$\cos\gamma_0^o(h) = c_2/(1+h)\sqrt{u_0^o(h)} \tag{7}$$

$$\psi_0^o(h) = c_3 \tag{8}$$

$$P_{u0}^o(h) = -a_2/2u_0^o + a_1 \tag{9}$$

$$P_{r0}^o(h) = a_2\tan\gamma_0^o \tag{10}$$

$$P_{\psi 0}^o(h) = a_3 \tag{11}$$

The subscript zero denotes the fact that these are the zero-order solutions in the expansion variable $\varepsilon = 1/\beta r_s$, and the superscript $o$ denotes outer solution.

The dimensionless variables $h$ and $u$ appearing above are defined in terms of the original dimensional state variables as

$$h = (r - r_s)/r_s, \qquad u = V^2/g_s r_s \tag{12}$$

Note that $h = 0$ at the reference radius and that $h$ is used as the independent variable in the original problem definition and in the outer solution.

In the inner region, where the aerodynamic force is dominant, a new stretched altitude $\eta$ and state variables $w$ and $v$ are defined as

$$w = Be^{-\eta}, \qquad \eta = h/\varepsilon, \qquad B = C_L^*\rho_s s/2m\beta \tag{13}$$

$$v = E^*\ell_n(1/g_s r_s u), \qquad E^* = C_L^*/C_D^* \tag{14}$$

Presented as Paper 92-4454 at the AIAA Guidance, Navigation, and Control Conference, Hilton Head, SC, Aug. 10–12, 1992; received Feb. 27, 1993; revision received July 1, 1994; accepted for publication July 22, 1994. Copyright © 1994 by the American Institute of Aeronautics and Astronautics, Inc. All rights reserved.

*Post Doctoral Fellow, School of Aerospace Engineering. Member AIAA.
†Professor, School of Aerospace Engineering. Fellow AIAA.

In the above expressions $V$ is the velocity, $r$ is the radius from Earth's center, $g$ is the gravitational acceleration, $\rho_s$ is the reference air density at $r = r_s$, $s$ is the reference area, $m$ is the mass, and $C_L^*$ and $C_D^*$ are the lift and drag coefficients corresponding to the maximum lift-to-drag ratio. The reference radius corresponds to the lowest altitude of the trajectory.

The zero-order equations for the inner problem can be obtained by expressing the system in Eqs. (1–3) in terms of the inner variables appearing in Eqs. (13) and (14) and simply taking the limit as $\varepsilon$ approaches zero on the right-hand sides. The general solution for the inner system to zero order in $\varepsilon$ is given by

$$\gamma_0^i(\psi_0^i) = -k_1\psi_0^{i^2}/2 + k_2\psi_0^i + k_3 \tag{15}$$

$$w_0^i(\psi_0^i) = \left[k_1\psi_0^{i^3}/6 - k_2\psi_0^{i^2}/2 - k_3\psi_0^i + k_4\right]/\sigma \tag{16}$$

$$v_0^i(\psi_0^i) = (\sigma + 1/\sigma)\psi_0^i + \sigma\left[\left(\psi_0^i k_1 - k_2\right)^3\right]/3k_1 + k_5 \tag{17}$$

and

$$P_{0\gamma}^i(\psi_0^i) = \left(P_{0w}^i/\sigma\right)\psi_0^i + c \tag{18}$$

$$P_{0w}^i = \text{const}, \qquad P_{0v}^i = \text{const} \tag{19}$$

where

$$k_1 = P_{0w}^i/2\sigma^2 P_{0v}^i, \qquad k_2 = -c/2\sigma P_{0v}^i \tag{20}$$

The superscript $i$ in the above equations denotes that a variable is associated with the inner expansion. Note that for the inner problem $\psi$ is used as the independent variable.

The inner variables $w$ and $v$ are related to the outer variables $h$ and $u$ by the transformations in Eqs. (13) and (14). The outer solution costate variables can be expressed in terms of the corresponding inner solution costate variables using

$$P_{0u}^i = P_{0v}^i \frac{\partial v}{\partial u}\bigg|_0^i = -\frac{E^* P_{0v}^i}{u_0^i} \tag{21}$$

where $\sigma$ is the normalized horizontal lift component given by

$$\sigma = 1/\left(1 + k_2^2 + 2k_1k_3\right)^{1/2} \tag{22}$$

A uniformly valid zero-order approximation for the optimal solution is constructed by adding the outer and inner solutions and subtracting their common parts:

$$x_0^c(h, \varepsilon) = x_0^o(h) + x_0^i(h/\varepsilon) - x_0^c(0) \tag{23}$$

The superscript $c$ is used to denote this composite solution, and $x$ is used to denote any of the variables of interest. Note that the composite solution must have $h$ as the independent variable to be consistent with the original MAE problem formulation. Also note that the matching conditions require

$$x_0^o(0) = x_0^i(\infty) \tag{24}$$

and that the boundary conditions are satisfied using the composite solution. The limit values in Eq. (24) also define the common parts of the inner and outer solutions.

The entry and exit Keplerian arcs (outer solution) are different in their orbital parameters. Thus there are two separate outer solutions (called the left and right solutions in Ref. 1). In total, there are 18 integration constants (12 from the two outer solutions and 6 from the inner solution) that need to be evaluated to obtain a composite solution. The reference radius $r_s$ and the horizontal component of lift $\sigma$, which was shown to be constant to zero order in $\varepsilon$, bring the total number of unknowns to 20. The left and right matching conditions and the boundary conditions for the composite solution provide 18 algebraic equations. Two additional equations are obtained by using $H_\sigma = 0$ [Eq. (22)] and the fact that $r = r_s$ when $\gamma_0^c(0, \varepsilon) = 0$. This gives a total of 20 coupled algebraic relations between the constants, and an iterative method is needed to calculate them.

In the next section we show how to simplify the original problem by exploiting the structure of the MAE solution procedure. This results in reducing the problem to a set of six implicit equations in six unknowns. In addition, a nested iteration process is developed so that two of the boundary conditions are always satisfied in each outer loop iteration. Thus, the outer loop iteration is further reduced to solving four equations in four unknowns.

## III. Zero-Order MAE Solution Procedure

The vehicle used in this study is the maneuverable research reentry vehicle (MRRV). Its aerodynamic and mass characteristics are presented in Ref. 2. The maximum lift-to-drag ratio is 2.362, the lift coefficient corresponding to $(L/D)_{\max}$ is $C_L^* = 0.1512$, the reference area is $s = 11.69\ \text{m}^2$, and the mass is $m = 4898.7$ kg. The constants needed for the exponential atmospheric density function were obtained by fitting to the standard atmosphere densities at 30 and 60 km. The resulting value of the scale height is $H_s = 1/\beta = 7625.4$ m.

A Newton method was first tried to solve for the 20 unknowns. This approach was not successful due to the complexity of the relations. An alternative approach was then derived wherein the number of coupled equations was reduced to 6 by defining the unknowns to be the common parts of the separate inner and outer solutions. The equations that determine these unknowns are the original boundary conditions enforced on the composite solutions. The basic idea is to first use the common parts as artificial boundary conditions to evaluate the constants of integration in Eqs. (6–11) and (15–20), starting with an initial guess. Then a Newton method is used to iterate on the common parts until the original boundary conditions are satisfied by the composite solution.

This procedure was slightly modified to capitalize on the structure of the MAE solution for this problem. Since $\psi_0^o$ is constant in the outer solution, it follows from Eq. (23) and the matching condition that $\psi_0^c$ (the composite solution for $\psi$) is simply the zero-order inner solution ($\psi_0^i$). This allows the boundary conditions on $\psi$ to be enforced using only the inner solution at each stage of the iteration process. Nested Newton iteration algorithms were implemented to determine the six unknowns using the boundary conditions for the composite solution. The inner iterations procedure corresponds to solving the inner problem with the boundary conditions on $\psi$ enforced. The outer iteration process is used to enforce the four remaining boundary conditions on the composite solution.

The first step in the procedure is to calculate the six inner solution integration constants $k_3$, $k_4$, $k_5$, $P_{0w}^i$, $c$, and $P_{0v}^i$ in Eqs. (15–20) using a guess for the common part values of $\gamma_0^i$, $v_0^i$ on the left and for the common part values of $\gamma_0^i$, $P_{0v}^i$ on the right (the constants $k_1$ and $k_2$ are known in terms of the other constants). Note that an initial guess for the common parts of $w_0^i$ is not needed since the common part corresponds to $\eta \to \infty$. Hence it follows from Eq. (13) that the common-part values for $w_0^i$ are zero on both the left and right sides. This particular arrangement concerning which of the common-part values are treated as unknowns was chosen to agree with the actual boundary conditions for the original problem, which greatly simplifies the problem of forming an initial guess. The procedure for forming an initial guess and the equations for evaluating the constants of integration are given in the Appendix.

Next, an inner loop Newton iteration is performed on the left and right common-part values of $\psi_0^i$ (using only the inner solution) so that the boundary conditions $\psi_0^i(w_i) = \psi_i$ and $\psi_0^i(w_f) = \psi_f$ are satisfied, where $w_i$ and $w_f$ correspond to $r = r_i$ and $r = r_f$ in Eq. (13). This is done by solving the cubic equation in Eq. (16) while taking into account that $w_0^i(\psi)$ for the range of $\psi$ of interest must be positive for the solution to have physical meaning. The inner solution procedure also determines $r_s$ and $\sigma$ (see the Appendix).

Figure 1 presents an example converged solution of this equation for $\psi_i = 0$ deg, $\psi_f = 20$ deg. The resulting left and right common parts of $\psi_0^i$ are $-1.10$ deg and 20.75 deg, respectively, which correspond to $w_0^i = 0(\eta \to \infty)$ in this figure. The values of $w_0^i$ at $\psi = 0$ deg and $\psi = 20$ deg map to $z_i = z_f = 60$ km altitude above sea level via Eq. (13). These altitudes were specified as part of the boundary conditions. Thus the boundary conditions $\psi_i(r_i) = 0$ deg and $\psi_f(r_f) = 20$ deg have been met.

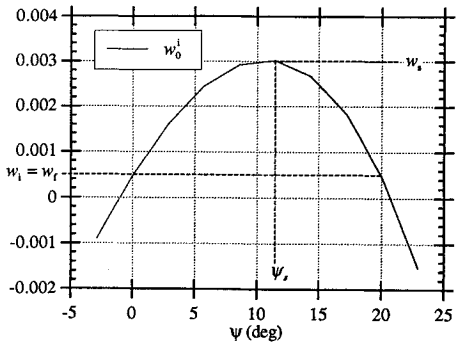


**Fig. 1 Example of converged inner Newton iteration for $w_0^i$ as a function of $\psi$.**

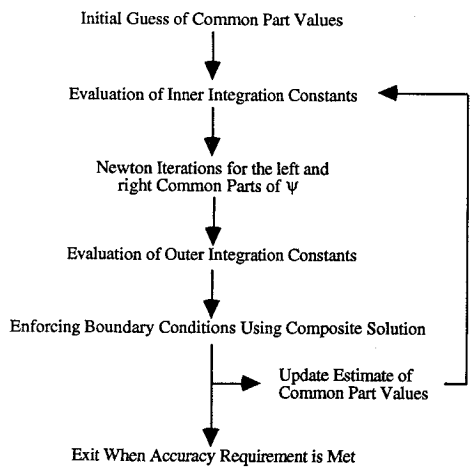


**Fig. 2 Summary of numerical solution procedure.**

The left and right outer solution integration constants in Eqs. (6–11) are obtained by enforcing the matching conditions in Eq. (24). This amounts to equating the common parts for the outer solution [Eqs. (6–11) evaluated at $h = 0$] with the common parts from the inner solution [Eqs. (15–20) evaluated at the left and right common-part values of $\psi_0^i$ corresponding to $w_0^i = 0$ in Fig. 1]. Since some of the outer solution variables are different from the inner solution variables, it is necessary to employ the transformations in Eqs. (13), (14), and (21). Note that $c_3$ and $a_3$ are not needed since the outer solutions for $\psi_0^o$ and $P_{\psi 0}^o$ are constant. Hence the composite solution for these variables is the inner solution alone. The composite solution is then evaluated to determine if the boundary conditions are satisfied:

$$\begin{aligned} u_0^c(h_i) - u_i &= 0, & \gamma_0^c(h_i) - \gamma_i &= 0 \\ P_{u0}^c(h_f) - 1 &= 0, & \gamma_0^c(h_f) - \gamma_f &= 0 \end{aligned} \tag{25}$$

The error in these equations is used in an outer loop Newton iteration to iterate on the remaining four unknown common parts. These are the left common-part values for $u$ and $\gamma$ and the right common-part values for $P_u$ and $\gamma$. A summary of this procedure is given in Fig. 2.

## IV. Numerical Results

**Open-Loop Solution**

Figures 3 and 4 present the zero-order MAE converged solution for the boundary conditions: $z_i = z_f = 60$ km (initial and final altitudes above sea level), $V_i = 7851$ m/s, $\gamma_i = -1.35$ deg, $\gamma_f = 1.0$ deg, and $\Delta\psi = 20$ deg. The corresponding altitude history is given later in Fig. 9 and the control time histories are given in Figs. 10 and 11 together with the optimal and the zero-order guided solutions. The value of the expansion parameter used here is $\varepsilon = 1/\beta r_s = 11.87 \times 10^{-4}$. Similar results were obtained at other heading changes between 10 deg and 40 deg. In Figs. 3 and 4 the inner solution is shown for the complete range of $\psi$ between its left and right common-part values, which correspond to $\eta = \infty$ ($w_0^i = 0$ in Fig. 1). This was done to illustrate the fact that the matching conditions in Eq. (24) are satisfied on the left and right portions of the solution.

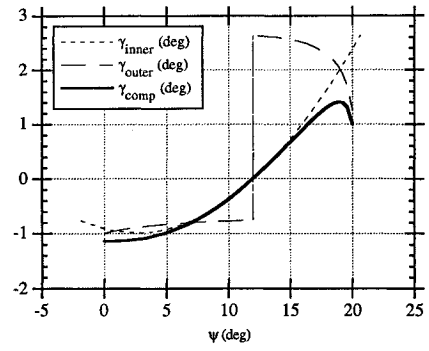


**Fig. 3a Zero-order MAE inner, outer, and composite $\gamma$ solution.**

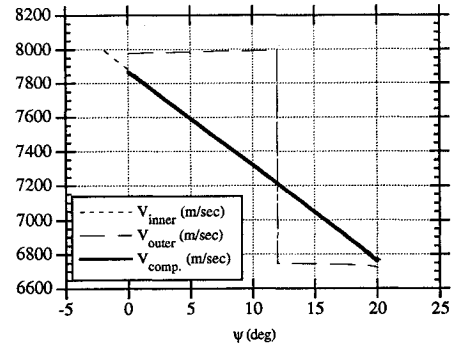


**Fig. 3b Zero-order MAE inner, outer, and composite velocity solution.**

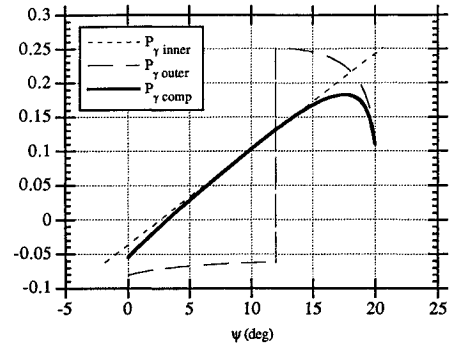


**Fig. 4a Zero-order MAE inner, outer, and composite $P_\gamma$ solution.**

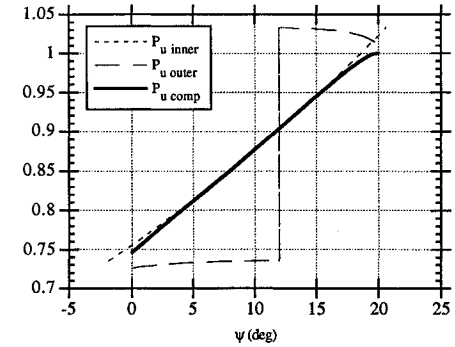


**Fig. 4b Zero-order MAE inner, outer, and composite $P_u$ solution.**

These results clearly indicate that the composite solutions for $\gamma$ and $p_\gamma$ are significantly different from the inner solution. In particular, the major variation in $p_\gamma$ is due to the outer solution, which (as explained in Ref. 1) in effect amounts to a correction for the large variation in Loh's term during the exit phase. The implications of this important correction have been fully addressed in Ref. 1 and will not be elaborated here. However, we do note that the outer solution plays an important role in forming a uniformly valid zero-order approximation to the exact solution. The normalized lift control $\lambda$ is always near 1.0, corresponding to

flight at near-maximum lift-to-drag ratio. The bank angle $\mu$ is near 90 deg, indicating that most of the aerodynamic force is utilized in performing the turn.

**Guided Solution**

Closed-loop guided solutions are obtained by using the optimal-control expressions given in Eq. (5). These expressions involve both the states and the costates; thus knowledge of both states and costates is needed to evaluate the controls. Assuming that the states are available for feedback, only estimates of the costates are required at each control computation along the trajectory. Feedback implementation entails treating the current state (from the simulation) at each control update as a new initial state and calculating the costate values corresponding to the same time instant. The estimate for these costates (to zero order) are obtained by repetitively solving the zero-order MAE problem.

At the first step, an initial guess and boundary conditions are supplied to initiate the procedure of obtaining a zero-order MAE converged solution (Appendix). Next, the costate expressions in Eqs. (9–11) and (18–20) can be evaluated as a function of the corresponding independent variables and used in Eq. (23) to construct the composite costate expressions. These are in turn used in Eq. (5) to compute the controls. When a predetermined time increment has been reached, the current states are used as initial conditions for the next MAE calculation. It follows that the initial guess is available in every step of the zero-order MAE calculation after the first.

For control computation between MAE solution updates, the integration constants from the last update are used. The transformations defined in Eqs. (12–15) are used to transform the simulated dimensional variables into the inner and outer dependent and independent variables. The transformed altitude $h$ is used in Eqs. (6), (7), (9), and (10) to compute the left and right outer costates. The heading $\psi$ is used in Eq. (18) to evaluate $P_\gamma$, and Eq. (23) is used to calculate the composite costates. The composite costates and the current $\gamma$ and $u$ [from Eq. (12)] are used in Eq. (5) to evaluate the optimal controls between the time instants where the MAE solution is updated.

During the exit phase, the left outer solution is discarded, and matching is required only between the right outer solution and the inner solution. In this case, the constants of integration for the inner solution are viewed as free parameters to satisfy the boundary conditions.

Figures 5–9 present a comparison between the optimal solution (obtained using a multiple shooting method[4]) and the zero-order guided solution for $\Delta\psi = 20$ deg with the open-loop altitude history added in Fig. 9. The corresponding control time histories are given in Figs. 10 and 11 together with the open-loop controls. Loh's term (corresponding to the optimal solution) is given in Fig. 12. The time increment between MAE solution updates is 5 s, with the control updated at every integration step following the procedure described above. These results indicate that the guided solutions and the optimal solutions are in a very good agreement throughout the trajectory. The error that does exist in some of the guided-solution variables, for example the $\gamma$ and the altitude ($z$) solutions, indicate the need for a first-order correction. A general procedure for MAE expansion of the Hamilton–Jacobi–Bellman equation to first order is developed in Ref. 3, along with its application to aeroassisted orbit transfer.

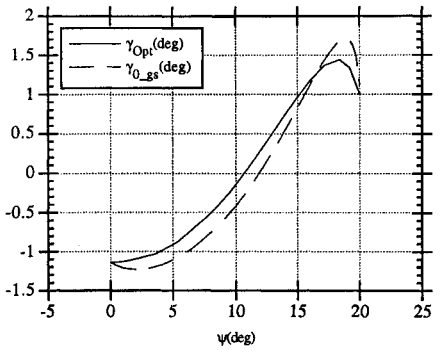


**Fig. 5 Optimal and guided $\gamma$ solutions.**

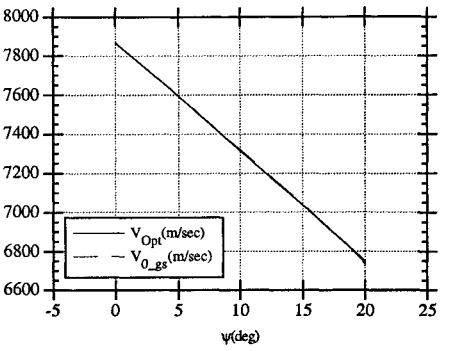


**Fig. 6 Optimal and guided velocity solutions.**

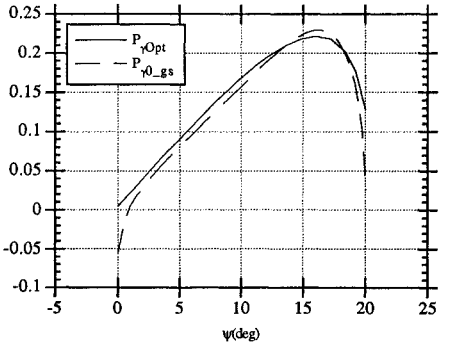


**Fig. 7 Optimal and guided $P_\gamma$ solutions.**

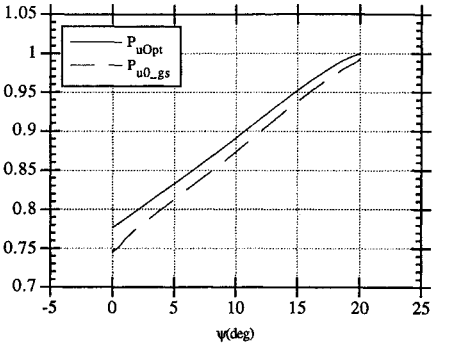


**Fig. 8 Optimal and guided $P_u$ solutions.**

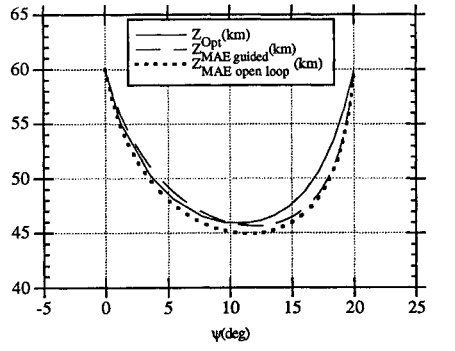


**Fig. 9 Optimal, guided, and open-loop altitude solutions.**

Figures 7 and 10 clearly indicate how the variation in Loh's term near the end of the trajectory is partially accounted for in the zero-order guided solution. Specifically, the normalized lift coefficient $\lambda$ given in Fig. 10 does not saturate in the exit phase but reduces to near zero. This is due to the fact that the correction in $P_\gamma$ from the outer solution is too large (see also Fig. 4a). Figure 13 compares the velocity histories near the end of the trajectory. The optimal- and guided-solution values for terminal velocities are 6751 and 6736 m/s, respectively. The difference of the guided value from the optimal one is 15 m/s.

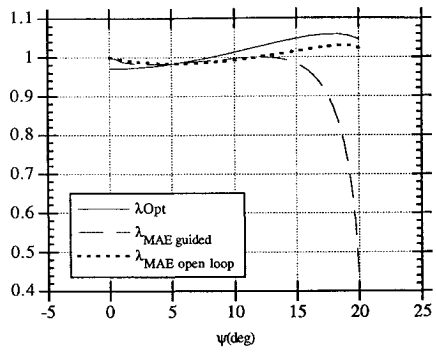


**Fig. 10 Optimal, guided, and open-loop normalized lift control.**

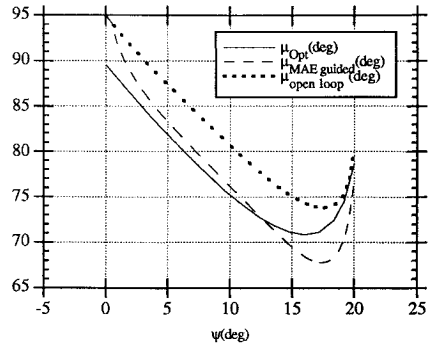


**Fig. 11 Optimal, guided, and open-loop bank angle control.**

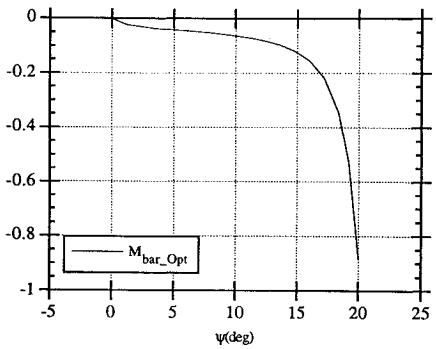


**Fig. 12 Optimal Loh's term variation.**

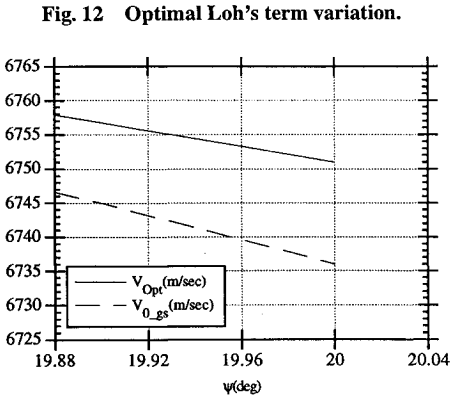


**Fig. 13 Optimal and guided performance.**

## V. Conclusions

Matched asymptotic analysis of aeroassisted inclination change with minimum energy loss leads to a coupled system of algebraic equations with 20 unknowns. By exploiting the structure inherent in the matching procedure, it is possible to significantly reduce the computational complexity and effort needed to solve these equations. Numerical experience shows that the zero-order solution is close to the optimal solution and that the outer solution plays a critical role in accounting for the variations in Loh's term near the exit phase of the maneuver. However, the deficiency that remains in several of the critical variables indicates the need for a first-order correction.

## Appendix: Estimation of Inner Integration Constants

To calculate the six inner integration constants $k_3$, $k_4$, $k_5$, $P^i_{w0}$, $c$, and $P^i_{v0}$ in Eqs. (15–20), six boundary values must be supplied. These are the left common-part values of $\gamma$, $v$, and $\psi$ and the right common-part values of $\gamma$, $P_v$, and $\psi$, which will be denoted by subscript $L$ and $R$, respectively. From Eq. (13) at $\eta \to \infty$, the common-part values of $w$ are zero; thus $w_L = w_R = 0$. The actual left boundary values of $\gamma$, $v$, and $\psi$ and the right boundary value of $\gamma$ and $\psi$ are used as an initial guess for $\gamma_L$, $v_L$, $\psi_L$, $\gamma_R$, and $\psi_R$, respectively. The value of $P_{vR}$ is estimated using the boundary condition that $P^o_{u0}(h_f) = 1.0$ [corresponding to maximizing $u(h_f)$] and the matching condition $P^o_{u0}(0) = P_{vR}$. Note that $P^i_v$ is constant; hence the composite costate $P^o_{u0}(h, \varepsilon)$ is equal to the outer costate $P^o_{u0}(h)$.[1]

Using Eqs. (15) and (16) at the left and right boundary conditions, $k_1$, $k_2$, and $k_3$ become

$$k_1 = -12\sigma \frac{\Delta w}{\Delta\psi^3} - \frac{6(\gamma_R + \gamma_L)}{\Delta\psi^2} \tag{A1}$$

$$k_2 = \frac{\Delta\gamma}{\Delta\psi} + \frac{k_1(\psi_R + \psi_L)}{2} \tag{A2}$$

$$k_3 = -\frac{k_1\psi_R\psi_L}{2} + \frac{\gamma_L\psi_R - \gamma_R\psi_L}{\Delta\psi} \tag{A3}$$

where $\Delta(\cdot) = (\cdot)_R - (\cdot)_L$. Use of Eqs. (A1) and (A2) and the estimate of $P^i_v$ in Eq. (20) provides the values of the constants $P^i_{w0}$ and $c$. In Ref. 1 it was shown that

$$\sigma^2 = 1/\left(1 + k_2^2 + 2k_1k_3\right) \tag{A4}$$

Next, $k_4$ and $k_5$ can be found using Eqs. (16) and (17) at the left boundary conditions:

$$k_4 = \sigma w_L - k_1\psi_L^3/6 + k_2\psi_L^2/2 + k_3\psi_L \tag{A5}$$

$$k_5 = v_L - (\sigma + 1/\sigma)\psi_L - \sigma\left[(\psi_L k_1 - k_2)^3\right]/3k_1 \tag{A6}$$

At this stage all the inner states and costates can be evaluated at any $\psi$ between $\psi_L$ and $\psi_R$ as a function of the boundary conditions using Eqs. (15–20). In particular, the initial and final inner solutions are needed to construct the composite solution, which is used to enforce the boundary conditions. Also, at the lowest point in the trajectory ($h = 0, r = r_s$) the composite solution is equal to the inner solution and the flight path angle is zero.[1] Thus, the value of $\psi_s$ that corresponds to this point can be found from Eq. (15) by equating it with zero and then using the result in Eq. (16) to calculate the corresponding value of $w_s$. This point is illustrated in Fig. 1. Finally, $\rho_s$ and hence the reference radius $r_s$ can be obtained by using $w_s$ and the relationships defined in Eq. (13).

## Acknowledgments

This research was supported by NASA Langley Research Center under Grant NAG-1-1139. The NASA technical monitor is Dan Moerder.

## References

[1]Calise, A. J., and Melamed, N., "Optimal Guidance of Aeroassisted Transfer Vehicles Based on Matched Asymptotic Expansions," *Journal of Guidance, Control, and Dynamics*, Vol. 18, No. 4, 1995, pp. 709–717.

[2]Hull, D. G., and Speyer, J. L., "Optimal Reentry and Plane Change Trajectories," *Journal of the Astronautical sciences*, Vol. 30, 1982, pp. 117–130.

[3]Calise, A. J., and Melamed, N., "Matched Asymptotic Expansion of the Hamilton-Jacobi-Bellman Equation for Aero-assisted Plane-Change Maneuvers," *Proceedings of the AIAA Guidance, Navigation, and Control Conference* (Monterey, CA), AIAA, Washington, DC, 1993, pp. 456–465 (AIAA Paper 93-3752).

[4]Oberle, H. J., and Grimm, W., "BNDSCO—A Program for the Numerical Solution of Optimal Control Problems," English Translation of DFVLR-Mitt. 85-05, DLR, German Aerospace Research Establishment, Oberpfaffenhofen, Germany.